Journal of Ecosystem Science and Eco-Governance (JESEG)

Vol. 7, No. 1 | June 2025
PRINT ISSN 2704 4394 | ONLINE ISSN 2782 8522
DOI: https://doi.org/10.54610/jeseg.v7i1.139

Assessing Land Cover Change and Flood Exposure from River Embankment Using GIS and Remote Sensing for Sustainable River Management: A Case Study of the Tumampit River in Ampayon, Butuan City, Philippines

Arnaldo C. Gagula[1,4], Stephanie Mae Salcedo-Albores[2,4], Jun Love E. Gesta[1,4], Marlon V. Elvira[3,4]*

[1]Department of Geodetic Engineering, College of Engineering and Geosciences, Caraga State University,
[2]Department of Civil Engineering, College of Engineering and Geosciences, Caraga State University,
[3]Department of Environmental Science, College of Forestry and Environmental Science, Caraga State University,
[4]Caraga Center for Geo-informatics, Caraga State University, Butuan City, 8600, Philippines

*Corresponding Author
*Email: acgagula@carsu.edu.ph
Received: October 14, 2024
Revised: May 15, 2025
Accepted: May 16, 2025
Available Online: June 16, 2025

Copyright © June 2025, Caraga State University. This is an open access article distributed under the Creative Commons Attribution License, which permits unrestricted use, distribution, and reproduction in any medium, provided the original work is properly cited.

Cite this article: Gagula, A.C., Albores, S.M.S., Gesta, J.L.E. & Elvira, M.V. (2025). Assessing Land Cover Change and Flood Exposure from River Embankment Using GIS and Remote Sensing for Sustainable River Management: A Case Study of the Tumampit River in Ampayon, Butuan City, Philippines, *Journal of Ecosystem Science and Eco-Governance*, **7**(1):20-35. DOI: https://doi.org/10.54610/jeseg.v7i1.139

ABSTRACT

This research assessed the environmental and social effects of the Tumampit River Embankment Project in Ampayon, Butuan City, Philippines, built between 2018 and 2022 to address flooding and riverbank erosion. With GIS-based analysis, land cover transformation and flood exposure were evaluated based on the comparison of 2018 (pre-embankment) and 2023 (post-embankment) data of an 82.13-hectare subwatershed with 728 structures in 2018, rising to 881 in 2023. Findings indicated a great conversion of natural land cover to built-up land. An estimated 73,500 m² of agricultural land and 42,800 m² of forest cover were converted into urban use during 2018-2023, while built-up land increased by 111,000 m². In spite of flood control, built-up areas continued to be the most flood-exposed land cover and were exposed to as much as 376,870 m² under the 100-year return period with the embankment in existence. Flood simulation indicated decreased areas of inundation for all but the highest hazard levels. In the 5-year event, the embankment lowered low-level flood exposure by 4,080,000 m². Under the 100-year event, exposure to moderate and high flood levels increased within urban areas, indicating spatial real location of flood hazards. In 2023, 303 structures were still exposed to low-level floods under the 5-year event and 549 structures under the 100-year event, compared to 498 and 619 structures, respectively, without the embankment. Although the embankment was effective in curbing flood extent in certain locations, it also had an effect on land cover conversions and continued exposure of developed areas to higher flood levels. The results highlight the intricate trade-offs between urban growth and ecosystem integrity, reminding us to incorporate land use planning and ecological measures into future flood control policies.

Keywords: *Flood Control, Land Cover, River Embankment, Flooding*

1 Introduction

River systems are the lifeblood of landscapes, providing essential ecological, economic, and social services that promote human well-being and environmental sustainability (Tiwari et al. 2003). Nevertheless, these dynamic systems face growing pressures from anthropogenic activities like urbanization, agricultural expansion, and infrastructure development. These alterations interfere with natural flow regimes, sediment transport, and riparian habitats, compromising river health and long-term community resilience (Zamroni et al. 2020).

For the Philippines, rivers play a unifying central function in supporting livelihoods, heritage, and environmental security. The tension between conservation and development is particularly difficult in the case of highly populated or fast-growing areas (Salvaña & Arnibal 2019). Sustainable river management means, therefore, having a profound sense of such trade-offs so that infrastructural interventions do not compromise ecological integrity.

Among the most prevalent river engineering structures are embankments, constructed for flood mitigation and riverbank stabilization. Although effective in minimizing near-term flood risks, these structures can radically change river dynamics and create unforeseen environmental and socio-economic impacts (Ogilvie et al. 2025). For example, flow velocity changes and channelization tend to downgrade aquatic habitats and biodiversity, with disturbance of sediment transport possibly leading to downstream erosion and decreased fertility of the floodplains (Wohl et al. 2019, Jähnig et al. 2023, Wang et al. 2021).

Urbanization further exaggerates these effects by substituting vegetated floodplains with impermeable coverings, increasing runoff and flood susceptibility. To counter, combined measures such as river restoration and spatial surveillance are becoming increasingly prominent as vital mesures of developing resilient urban landscapes (Voulvoulis et al. 2024, Calheiros et al. 2021).

Flooding is one of the Philippines' most enduring risks, and it continues to pose a significant threat in low-lying and riverine zones such as Butuan City. To counter recurrent flood occurrences and safeguard infrastructures of vital importance, structural countermeasures have been executed. Among these interventions is the Tumampit River Embankment in Barangay Ampayon, Butuan City—a 780.80 m. concrete embankment constructed from 2018 to 2022 to regulate flooding and shore protection along a critical stretch of the Tumampit River.

Although intended for protection, embankments can promote land cover change and modify flood exposure patterns. Vegetated strips can be transformed into urbanized areas, hence enhancing localized risk. Still, after-construction assessments of em-bankment projects within the Philippines are rare—particularly studies that apply spatial analysis to determine environmental and disaster-related effects.

This research aims to bridge that gap by examining land cover change and flood exposure along the Tumampit River Embankment. Employing GIS and remote sensing, the study contrasts spatial data across pre- and post-embankment years (2018 and 2023), analyzes land use change, simulates flood scenarios, and evaluates the performance of the embankment in flood risk reduction. It aims to provide insights for more sustainable and evidence-based river management.

Particularly, the research seeks to examine changes in land cover in the 821,300 sq.m. subwatershed to determine the stability or change of urban, agricultural, and vegetated zones; Quantify flood exposure under various return periods (5-year and 100-year cases) with and without a river embankment; and measure the reduction of flood-prone areas by the embankment and evaluate the residual vulnerability of built-up areas in spite of structural mitigation.

The research targets an 821,300 m² subwatershed along a 3,997.35-meter reach of the Tumampit River. Land cover detection is for urban, tree, crop, and rangeland. Flood exposure of each land class is estimated under simulated 5-year and 100-year return periods. The performance of the embankment is evaluated by comparing flood extents with and without the embankment.

However, the research confines itself to physical and spatial information and does not incorporate socio-economic or demographic vulnerability estimation. It employs existing models of floods from 2017 and does not take future climate projections into account. The analysis applies the ideal per-formance of the embankment and does not take structural depreciation or maintenance matters into consideration. Moreover, whereas built-up exposure is estimated, damage assessment and ground-truthing are outside the framework of the study.

2 Methodology

Study Area

Figure 1 shows the study area at Tumampit River, Barangay Ampayon, Butuan City. It has an area of 821,300 square meters or 82.13 hectares. In this study, we only focus on the sub-watershed area where the Tumampit River is located, with a river length of 3,997.35 meters.

Landcover Change and Analysis

The landcover maps of 2018 and 2023 were

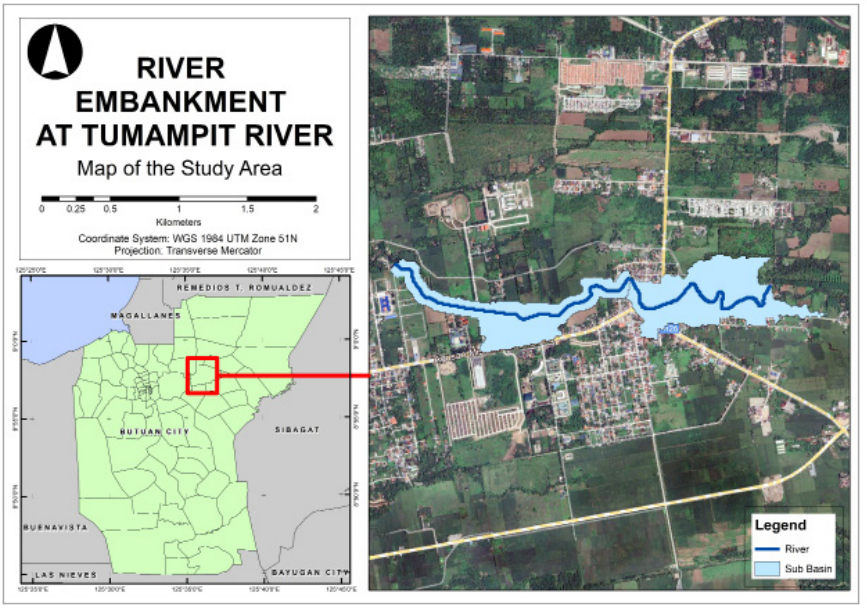

Figure 1. Map of the Study Area along Tumampit River in Brgy. Ampayon, Butuan City, Philippines

downloaded in July 2023 from the ArcGIS Living Atlas of the World (https://livingatlas.arcgis.com/en/home). It provides a detailed, accurate, and timely LULC map of the world derived from ESA Sentinel-2 imagery at 10m resolution. This data results from a collaboration between Esri, Impact Observatory, and Microsoft (Esri, Impact Observatory, & Microsoft, 2024). These landcover maps are generated using a deep learning AI land classification model that uses a massive training dataset of billions of human-labeled image pixels developed by the National Geographic Society. The LULC maps were clipped using the boundary of the Tumampit subwatershed. In 2018, it comprised trees, crops, built area, and rangeland, while in 2023, it comprised trees, crops, built area, rangeland, and bare ground.

The area of each class in LULC maps was computed and subtracted to determine the class changes from 2018 to 2023. For better analysis, the 2018 LULC was intersected with the 2023 LULC to identify the conversion of each class.

Watershed Delineation

The delineation procedure follows the three major processes: Terrain Preprocessing, Project Set-Up, and Basin Processing. This was conducted to determine the boundaries of the watershed. The boundaries were identified by the topography of the study area, including the elevation, slope, and direction of the land surface.

Terrain Pre-processing

The reconditioned DEM enabled the elevation of the stream cells to be lowered, which was created through the utilization of the digitized river shapefile. One of the complications with the watershed cells is that some cells can trap water in a single cell, as each cell differs in elevation. The solution to this is the fill sink function. This study defined the elevation value of higher-elevation cells within the watershed's boundary. Flow direction followed this step, where each value of the grid in the cell was computed to know the direction of the steepest descent from the given cell. Next, the Flow Accumulation function allowed the calculation of the flow accumulation grid containing the gathered number of cells upstream of a particular cell. Another necessary function to implement was the stream definition which is a parameter that classifies streams in a cell that follows the detected flow accumulation value greater than the user value. The smaller values will have a greater number of delineated subbasins. The same grid code was assigned to cells that fall on a specific segment. The function of Stream Segmentation was employed to create the grid for the specific stream segment. With each stream segment identified,

Catchment Grid Delineation was also conducted to delineate each stream segment's subbasin. The computed catchment grid was then used for the next function. The Catchment Polygon Processing allows the catchment grid feature to be converted into a catchment polygon. With this function, a vector layer of the subbasins was created. Drainage Line Processing is another function that converts the stream grid into a line feature class. The feature class line has an individual identifier for where it is located. With this, another stream vector layer was created. The last function done as part of the major procedure was the Adjoint Catchment Processing. In this process, the drainage line and catchment processing data were used as input to combine the upstream catchment.

Project Set-up

This step in the delineation procedure was setting the project point, which is situated at the downstream outlet. This point was the project area for developing the Hydrologic Model using the HEC-HMS. Through HEC-GeoHMS, the upstream subbasin and rivers that are linked to the project point were delineated as well.

Basin Processing

This procedure is necessary for the polishing of the sub-basin delineation. In this step, the delineated sub-basins were enhanced. The option for dividing the sub-basins into smaller ones was also given. This function allowed the researchers to understand the hydrologic response at particular locations connected to the project area.

Analysis of Inundated Area

The lower Padsan River basin exhibits modThe Interferometric Synthetic Aperture Radar (IfSAR) Digital Elevation Model (DEM) was used as the input terrain data in HEC-RAS for simulating flood inundation. IfSAR-derived elevation data is widely used in flood modeling due to its high spatial resolution and ability to capture topographic variations critical for hydrologic and hydraulic analyses, even in vegetated or cloudy areas (Zandbergen, 2008). Several studies have demonstrated the reliability of IfSAR for delineating flood-prone areas and analyzing drainage networks, especially in large-scale or data-scarce regions (Sanders, 2007).

The Hydrologic Engineering Center River Analysis System (HEC-RAS), developed by the U.S. Army Corps of Engineers, is a robust, widely used modeling tool capable of performing one- and two-dimensional hydraulic simulations. It is particularly effective for assessing the impacts of river engineering structures, such as embankments and levees, on water surface elevations and flood extents (Horritt & Bates, 2002; Teng et al., 2017). HEC-RAS allows users to simulate flood behavior under different scenarios, evaluate structural interventions, and generate spatial outputs like flood depth, velocity, arrival time, and inundation dura-tion. This makes it well-suited for assessing how river embankment projects alter flood patterns and exposure in surrounding areas. The setup of the HEC-RAS interface for this study is shown in Figure 2.

The Elevation model incorporating the embankment was prepared in GIS by mosaicking the raster with the actual characteristics of the embankment. Shown in Figure 3 is the image showing the elevation model before(left) and after(right) the river embankment project.

The 5-year and 100-year rain return periods (T) were used to calculate the watershed's discharge. A 5-year return period rain event corresponds to a 20% probability of occurrence in any given year, while a 100-year return period event has a 1% annual probability. These return periods represent moderate and extreme rainfall scenarios, respectively, and were used to model flood inundation extents under varying conditions. The rain values (in millimeters) were based on the Rainfall Intensity Duration Frequency (RIDF) by the Philippine Atmospheric, Geophysical, and Astronomical Services Administration (PAG-ASA) (Table 1). As shown in the table, the 5-year return period is associated with a cumulative precipitation of 175.2 millimeters. Moreover, the 100-year return period rainfall data, with a cumulative total reaching 308.6 millimeters over 24 hours, indicates an extreme precipitation event that poses a high risk of widespread flooding.

The Hydrograph Output Interval in HEC-RAS (located under Unsteady Flow Analysis of the Computation Settings) refers to how frequently the model saves and displays results in the HEC-DSS file and Mapper, not how often internal calculations are performed. While the engine may compute flows every few seconds or minutes to maintain numerical accuracy, setting a 1-hour output interval is a strategic choice. It reduces data volume, keeps file sizes manageable, and supports smooth hydrograph visualization by averaging ungaged inflows over a

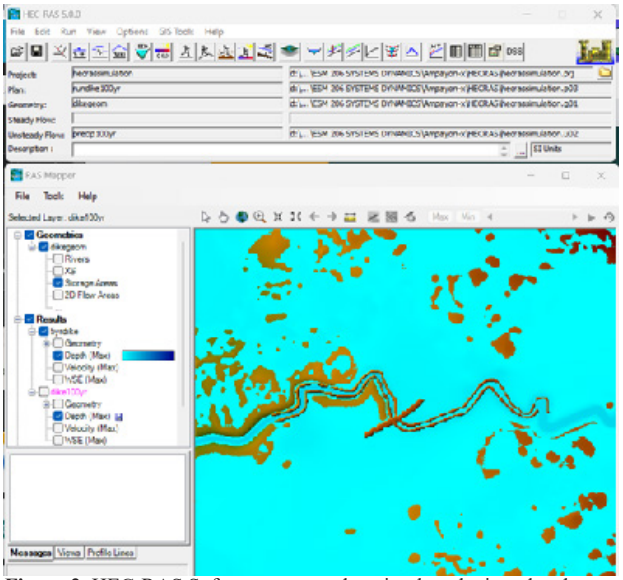

Figure 2. HEC-RAS Software was used to simulate the inundated area

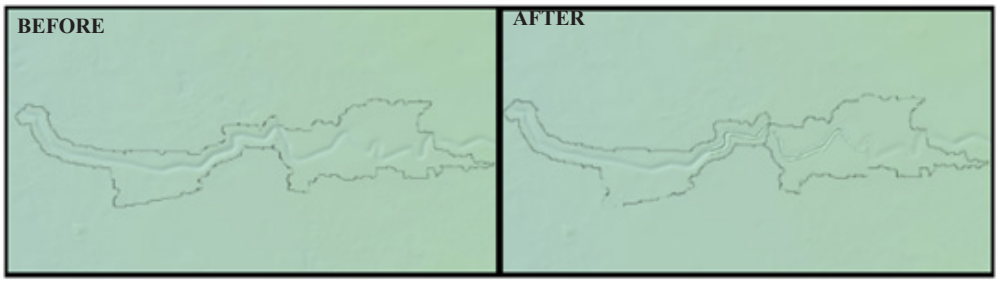

Figure 3. The image shows the elevation model of the area before and after the river embankment project.

Table 1. The level of flood hazard classification used in the study is based on its flood depth.

T(yrs)	5 mins	10 mins	15 mins	1 hr	2 hrs	3hrs	6 hrs	12 hrs	24 hrs
5	11.9	23.9	27.4	52.9	71.2	81.3	104.6	142.6	175.2
100	19.6	39.2	44.6	85.8	114	129.5	167.1	259.1	308.6

centered time window. This interval is particularly appropriate for planning studies where hourly data resolution is sufficient to capture flow behavior without overwhelming post-processing tasks (USACE, 2023). The setup of the interface of the HEC-RAS Model is shown in Figure 4.

Flood depth classifications in this study follow widely accepted thresholds used in hazard mapping and risk assessment. The classifications, as shown in the table, correspond to varying levels of impact on human safety and infrastructure. Depths of up to 0.5 m are generally considered low hazard but can still hinder pedestrian mobility, especially for vulnerable populations (ThinkHazard! Methodology, 2021). Floodwaters between 0.5 m and 1.0 m begin to pose risks to building integrity and vehicular movement (Vu, 2010). In the range of 1.0 m to 1.5 m, the potential for structural damage significantly increases, as supported by flood vulnerability studies that document a steep rise in damage ratios within this depth band (Xue et al., 2020). Depths exceeding 1.5 m are typically classified as high hazard, with increased risk to life, particularly in densely populated or poorly prepared areas (Vu, 2010; ThinkHazard! Methodology, 2021).

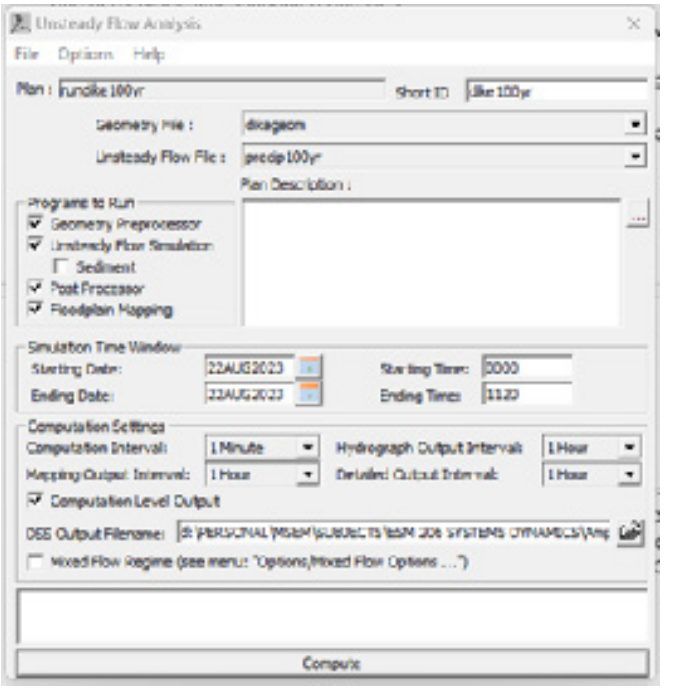

Figure 4. The interface of the HEC-RAS for Hydraulic Simulations.

3 RESULTS AND DISCUSSION

Land Cover Change and Analysis

Crops had the highest area in 2018 with 337,400 sq.m.; however, it is less with 39,600 sq.m. in 2023 (Figure 5). Also, negative changes can be observed in trees and rangeland, with an area of 80,600 sq. m. and 1,5400 sq. m., respectively. This means that trees, crops, and rangeland in 2018 were converted into other classes in 2023. On the other hand, an additional 111,000 sq.m. were added to the built area from 2018 to 2023.

There are 326,700 sq.m. for built area, 251,100 sq.m. for crops, 7,800 sq.m. for rangeland, and 36,600 sq.m. for trees, which were not converted to other classes (Figure 6; Table 3). Furthermore, 42,800 sq.m. of trees and 73,500 sq.m. of crops were converted into built-up areas. With 326,700 sq.m. of unchanged built area, urban zones exhibit stability despite flood risks. However, the shift of 73,500 sq.m. of crops and 42,800 sq.m. of trees to built-up areas underlines the pressure for urban expansion.

Flood Inundation Scenario Simulation

Table 4 summarizes the resulting flood levels, indicating the corresponding area in square meters for each hazard level. The 5-year scenario reduced values, showing a difference of 4,080,000 sq. m. between the two scenarios in the low level. Similarly, for the other levels, the values also decreased in the scenario with the embankment. The 100-year scenario also decreased values for all categories except the low flood level, although the difference is relatively minor. In general, the results demonstrated that the flood levels, in terms of the inundated area, experienced a decreasein the scenario with the embankment, a finding that aligns with previous studies on the effectiveness of structural flood mitigation measures (Wang et al. 2018, Lo et al. 2021). These findings reinforce the observed effectiveness of the Tumampit River embankment in mitigating flood exposure. Based on the results, there were 728 buildings within the boundary of the study area in 2018 and 881 buildings in 2023. These building footprints were initially obtained from the Phil-LiDAR-1 - Hazard Mapping of the Philippines using LiDAR and updated during the Geo-informatics for the Systematic Assessment of Flood Effects and Risks for a Resilient Mindanao (GeoSAFER) project datasets, which provide high-resolution spatial data for flood hazard mapping and exposure assessment. The tabulation of the affected buildings in 2018 under the 5-year and 100-year

Table 2. The level of flood hazard classification used in the study is based on its flood depth.

Depth Value	Hazard Level
0.01 to 0.5	Low
0.51 to 1.0	Medium
1.01 to 1.5	High
1.5 above	Very High

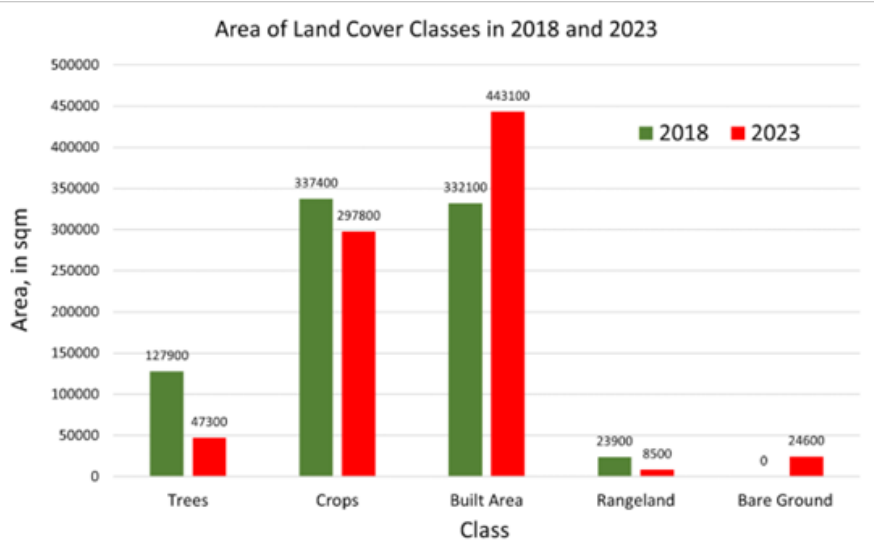

Figure 5. Area of land cover classes in 2018 and 2023.

flood hazard scenarios (Table 5 &6).

On the other hand, the tabulations of the results of the affected buildings of the year 2022 using the 5-year and 100-year flood hazards are shown in Tables 7 and 8, respectively.

Landcover Classes Affected by the Inundated Area

Based on the simulation without embankment, land cover classes in 2018 affected by 5-year and 100-year floods were computed and tabulated (Table 9 & 10). Based on the result, the Built Area is more exposed to flood in 5-year and 100-year scenarios, with an area of 229,130 and 274,392 square meters, respectively. While the least affected class was the rangeland, with an area of 17,257 sq.m. Moreover, crops are more exposed to very high flood levels for the two scenarios, with an area of 34,759 and 46,978 sq.m.

By computing land cover classes (Table 11 and 12), the results show that the built area is still the most exposed class to flood in the 5-year and 100-year scenarios, with an area of 215,662 and 376,870 sq.m., respectively.

Figure 7 is a bar graph showing the area affected by flood without an embankment (in 2018) and with the presence of an embankment (in 2023) for a 5-year scenario. In low flood levels, more built areas were affected in 2018 than in 2023. However, there are more affected areas in 2023 for the rest of the flood levels. For the 100-year flood scenario (Figure 8), built areas are more exposed to all flood levels in 2023 than in 2018. This suggests that, based on spatial modeling alone, built areas remain exposed to flooding even with the presence of an embankment. The visual comparisons in the figures indicate that the embankment had a varying impact on different flood levels. However, these results are derived from geospatial analysis and modeling and do not account for the actual physical condition, design, or performance of the embankment on the ground. Field validation, structural assessment reports, or flood impact studies would be necessary to confirm the effectiveness of the embankment in real conditions.

The Tumampit River Embankment Project is effective in minimizing the flood area under common and moderate flood intensities.

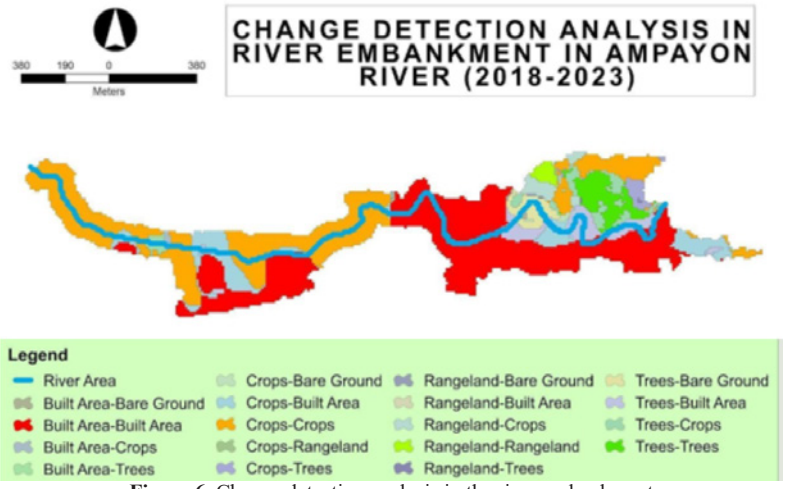

Figure 6. Change detection analysis in the river embankment.

Table 3. Changes of classes from 2018 to 2023 based on the change detection analysis.

2018	2023	Change	Area
Built Area	Bare Ground	Built Area-Bare Ground	1,900
Built Area	Crops	Built Area-Crops	3,100
Built Area	Built Area	Built Area-Built Area	326,700
Built Area	Trees	Built Area-Trees	400
Crops	Crops	Crops-Crops	251,100
Crops	Built Area	Crops-Built Area	73,500
Crops	Trees	Crops-Trees	9,800
Crops	Bare Ground	Crops-Bare Ground	2,300
Crops	Rangeland	Crops-Rangeland	700
Rangeland	Crops	Rangeland-Crops	14,900
Rangeland	Rangeland	Rangeland-Rangeland	7,800
Rangeland	Bare Ground	Rangeland-Bare Ground	600
Rangeland	Trees	Rangeland-Trees	500
Rangeland	Built Area	Rangeland-Built Area	100
Trees	Crops	Trees-Crops	28,700
Trees	Built Area	Trees-Built Area	42,800
Trees	Trees	Trees-Trees	36,600
Trees	Bare Ground	Trees-Bare Ground	19,800

Table 4. The area (in sq. m.) of specific hazard levels for 5-year and 100-year rain return flood hazards, with consideration of having and without embankment.

Hazard Level	5-Year (in sq. m.)		100-year (in sq. m.)	
	Without Embankment	With Embankment	Without Embankment	With Embankment
Low	17,190,000	13,110,000	17,230,000	17,390,000
Moderate	1,070,000	310,000	1,620,000	1,550,000
High	480,000	90,000	820,000	810,000
Very High	760,000	110,000	1,530,000	1,540,000

Table 5. Tabulation of affected buildings for the 5-year rain return flood hazard in the year 2018.

2018 Building Footprints		
5-year Flood Hazard	**Without Embankment**	**With Embankment**
Hazard Level	*No. of Household Affected*	
Low	407	249
Moderate	20	38
High	11	11
Very High	10	10
Not Flooded	280	420
Total	728	728

Table 6. The tabulation of affected households for the 100-year rain return flood hazard in the year 2018

2018 Building Footprints		
100-year Flood Hazard	**Without Embankment**	**With Embankment**
Hazard Level	*No. of Household Affected*	
Low	495	425
Moderate	35	131
High	25	48
Very High	28	22
Not Flooded	145	102
Total	728	728

Table 7. The tabulation of affected households for 5-year rain return flood hazard in the year 2023.

2023 Building Footprints		
5-year Flood Hazard	**Without Embankment**	**With Embankment**
Hazard Level	*No. of Household Affected*	
Low	498	303
Moderate	10	32
High	3	8
Table 7. The tabulation of affected households for 5-year rain return flood hazard in the year 2023.	10	10
Very High	15	11
Not Flooded	355	527
Total	881	881

Table 8. The tabulation of affected households for 100-year rain return flood hazard in the year 2023.

2023 Building Footprints		
100-year Flood Hazard	**Without Embankment**	**With Embankment**
Hazard Level	*No. of Household Affected*	
Low	619	549
Moderate	25	166
High	13	44
Very High	22	23
Not Flooded	202	99
Total	881	881

Nevertheless, flood threats in urban centers still exist, especially during rare events. The further encroachment of built areas into traditional natural and agri-cultural areas adds exposure and decreases the natural flood-modulating ability of the ecosystem. Geospatial modeling supports a reduction of inundated areas due to embankment, but, as per the paper, based only on models and has not yet been tested with field-based hydrological measurements or comparison of historical flood occurrences. Additional research involving ground-based flood data, structural performance analysis, and participatory risk assessment is advised to evaluate the long-term performance of the embankment and to inform sustainable land use and disaster risk reduction policy.

Table 9. Area of affected land cover classes (in sq. m.) for 5-year flood without embankment scenario.

Flood Level	Trees	Crops	Built Area	Rangeland
Low	74,574	132,410	188,743	15,878
Moderate	5,432	9,721	6,813	1,379
High	4,768	8,605	6,793	0
Very High	16,580	34,759	26,781	0
Sum	101,355	185,495	229,130	17,257
Total Inundated Area				**533,236.23**

Table 10. Area of affected land cover classes (in sq. m.) for 100-year flood without embankment scenario.

Flood Level	Trees	Crops	Built Area	Rangeland
Low	82,407	167,153	221,427	16,290
Moderate	8,670	14,639	9,691	2,244
High	5,242	9,120	7029	0
Very High	22,954	46,978	36,245	0
Sum	119,274	237,890	274,392	18,535
Total Inundated Area				**650,090.12**

Table 11. Area of affected land cover classes for the 5-year flood with embankment scenario.

Flood Level	Trees	Crops	Built Area	Rangeland	Bare Ground
Low	44,978	108,109	151,921	644	8,595
Moderate	479	11,888	18,485	0	4,561
High	127	8,502	10,752	0	510
Very High	86	8,114	34,504	0	3,683
Sum	4,5670	136,614	215,662	644	17,349
Total Inundated Area				**415,938.05**	

Table 12. Area of affected land cover classes (in sq. m.) for 100-year flood with embankment scenario.

Flood Level	Trees	Crops	Built Area	Rangeland	Bare Ground
Low	44,877	140,418	249,259	3,524	4,970
Moderate	1,893	22,480	61,973	0	6,546
High	343	6,971	18,400	0	4,176
Very High	165	31,149	47,238	0	4,122
Sum	47,278	201,017	376,870	3,524	19,814
Total Inundated Area				**648,503.13**	

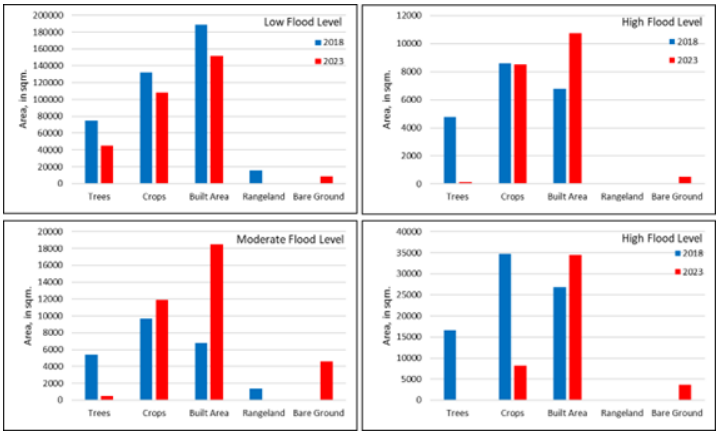

Figure 7. 2018 vs 2023 inundated area of land cover classes for 5-year flood scenario.

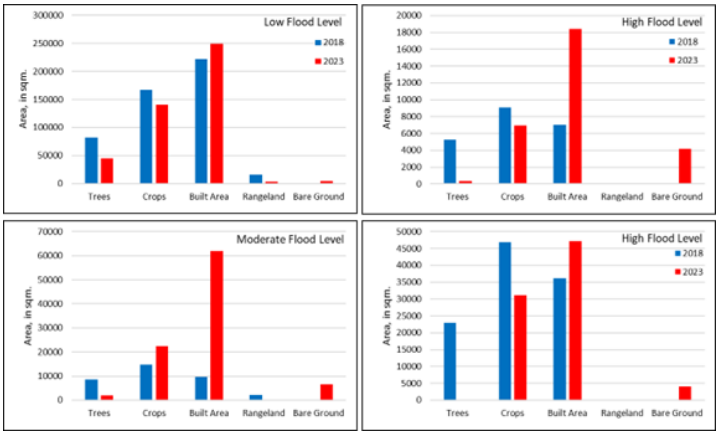

Figure 8. 2018 vs 2023 inundated area of land cover classes for the 100-year flood scenario.

4 Acknowledgment

The authors sincerely express their deepest appreciation to the barangay councils of Barangay Ampayon for granting permission to conduct this research activity. Special thanks are also extended to the local communities for their warm hospitality and support during the fieldwork phase.

The authors gratefully acknowledge their classmates—Jessan Desalago, Patch Buenavista, Gerome Amper, John Ebol, and Eric Doria—for their active participation and assistance in conducting this study.

5 Statement of Conflict of Interest

To ensure impartiality in the evaluation of this article, MV Elvira, a member of the JESEG Editorial Board, recused himself from the review process. The authors also declare that they have no competing financial interests or personal relationships that could have influenced the work presented in this paper.

6 Author Contribution

AC Gagula: Conceptualization, Methodology, Formal analysis, Investigation, Writing - Original Draft, Writing - Review and Editing, Supervision. SM Salcedo-Albores: Conceptualization, Methodology, Formal analysis, Investigation, Writing - Review and Editing. JLE Gesta: Conceptualization, Methodology, Formal analysis, Investigation, Writing - Review and Editing.

7 Literature Cited

Calheiros, C. T., de Azevedo Ribeiro, R. J., & Ferreira,F. A. (2021). River restoration integrated with sustainable urban water management for resilient cities. *Sustainability*, **12**(11), 4677. https://doi.org/10.3390/su12114677

Department of Public Works and Highways. (2020, January 24). Butuan City flood control project is now 89% completed. https://www.dpwh.gov.ph/dpwh/news/18072

Esri, Impact Observatory, & Microsoft. (2024, April 30). Annual 10-meter global land use/land cover maps available in ArcGIS Living Atlas of the World [Press release]. Esri Newsroom.

Flyriver. (n.d.). Environmental impacts of channelization. Retrieved from http://flyriver.gov.pg

Horritt, M. S., & Bates, P. D. (2002). Evaluation of 1D and 2D numerical models for predicting river flood inundation. *Journal of Hydrology,* **268**(1–4), 87–99.

Jähnig, S. C., Lorenz, A. W., Hering, D., & Antons, C. (2023). The effects of channelization with low in-stream barriers on macroinvertebrate communities of mountain rivers. *Water*, **15**(6), 1059. https://doi.org/10.3390/w15061059

Lo, W., Huang, C.-T., Wu, M.-H., Doong, D.-J., Tseng, L.-H., Chen, C.-H., & Chen, Y.-J. (2021). Evaluation of flood mitigation effectiveness of nature-based solutions potential cases with an assessment model for flood mitigation. *Water*, **13**(23), 3451. https://doi.org/10.3390/w13233451

Ogilvie, A., Fall, C. S., Bodian, A., Martin, D., Bruckmann, L., Dia, D., ... & Poussin, J. C. (2025). Surface water and flood-based agricultural systems: Mapping and modelling long-term variability in the Senegal river floodplain. *Agricultural Water Management*, **308**, 109254.

Sanders, B. F. (2007). Evaluation of on-line DEMs for flood inundation modeling. *Advances in Water Resources*, **30**(8), 1831–1843.

Teng, J., Vaze, J., Kinsey-Henderson, A., Lerat, J., & Wang, B. (2017). Future flood risk modelling: An overview. *Journal of Hydrology*, **550**, 331–345.

Salvaña, F. R. P., & Arnibal, S. L. T. (2019). Importance of indigenous communities' knowledge and perception in achieving biodiversity conservation: A case study from Manobo tribe of Southern Mindanao, Philippines. *Asian Journal of Ethnobiology*, **2**(2).

Tiwari, A. K., Singh, R., Kumar, S., & Singh, G. S. (2023). Ecosystem services in the riverine landscapes. In Advances in Water Resource Planning and Sustainability (pp. 273-303). Singapore: Springer Nature Singapore.

ThinkHazard! (n.d.). Flood hazard classification. Global Facility for Disaster Reduction and Recovery (GDRR).https://thinkhazard.org/en/report/227-philippines-flood

U.S. Army Corps of Engineers (USACE). (2023). HEC-RAS River Analysis System: User's Manual (Version 6.4). Hydrologic Engineering Center. https://www.hec.usace.army.mil/confluence/rasdocs/rasum/latest

Vu, P. H. (2010). Flood risk assessment for the Vu Gia-Thu Bon river basin in central Vietnam. UNE- SCO-IHE Institute for Water Education.

Voulvoulis, N., Arpon, K. D., & Giakoumis, T. (2024). Ecosystem services of urban rivers: A systematic review. *Aquatic Sciences*, **87**, 10. https://doi.org/10.1007/s00027-024-00915-2

Wang, X., Zhang, Z., & Liu, Y. (2021). Channel erosion and its impact on environmental flow of riparian habitat in the Middle Yangtze River. *Environmental Flow Reports*, **43**(2), 117–128.

Wang, Y.-H., Hsu, Y.-C., You, G. J.-Y., Yen, C.-L., & Wang, C.-M. (2018). Flood inundation assessment considering hydrologic conditions and functionalities of hydraulic facilities. *Water*, **10**(12), 1879. https://doi.org/10.3390/w10121879

Wohl, E., Lane, S. N., Wilcox, A. C., & Yarnell, S. M. (2019). River morphology, channelization, and habitat restoration. In River restoration in Mediterranean and other regional contexts (pp. 87–104). Springer.

Zandbergen, P. A. (2008). Applications of IfSAR for flood modeling in flat terrain. *International Journal of Geographical Information Science*, **22**(3), 301–319.

Zamroni, A., Putra, B. P., & Prasetya, H. N. E. (2020). Anthropogenic influences on morphological changes in the Progo River, Daerah Istimewa Yogyakarta Province, Indonesia. Sustinere: *Journal of Environment and Sustainability* **4**(3), 205-223.